ARMY RESEARCH LABORATORY

Structural Composite Supercapacitors: Electrical and Mechanical Impact of Separators and Processing Conditions

by Edwin B. Gienger, James F. Snyder, and Eric D. Wetzel

ARL-TR-6624 **September 2013**

NOTICES

Disclaimers

The findings in this report are not to be construed as an official Department of the Army position unless so designated by other authorized documents.

Citation of manufacturer's or trade names does not constitute an official endorsement or approval of the use thereof.

Destroy this report when it is no longer needed. Do not return it to the originator.

Army Research Laboratory
Aberdeen Proving Ground, MD 21005-5066

ARL-TR-6624 **September 2013**

Structural Composite Supercapacitors: Electrical and Mechanical Impact of Separators and Processing Conditions

Eric D. Wetzel and James F. Snyder
Weapons and Materials Research Directorate, ARL

Edwin B. Gienger
ORISE

REPORT DOCUMENTATION PAGE

Form Approved
OMB No. 0704-0188

1. REPORT DATE *(DD-MM-YYYY)*	2. REPORT TYPE	3. DATES COVERED (From - To)
September 2013	Final	June 2009–June 2012

4. TITLE AND SUBTITLE
Structural Composite Supercapacitors: Electrical and Mechanical Impact of Separators and Processing Conditions

5a. CONTRACT NUMBER
Orise 1120-1120-99

5b. GRANT NUMBER

5c. PROGRAM ELEMENT NUMBER

6. AUTHOR(S)
Edwin B. Gienger,* James F. Snyder, and Eric D. Wetzel

5d. PROJECT NUMBER
H42

5e. TASK NUMBER

5f. WORK UNIT NUMBER

7. PERFORMING ORGANIZATION NAME(S) AND ADDRESS(ES)
U.S. Army Research Laboratory
ATTN: RDRL-WMM-G
Aberdeen Proving Ground, MD 21005-5066

8. PERFORMING ORGANIZATION REPORT NUMBER
ARL-TR-6624

9. SPONSORING/MONITORING AGENCY NAME(S) AND ADDRESS(ES)

10. SPONSOR/MONITOR'S ACRONYM(S)

11. SPONSOR/MONITOR'S REPORT NUMBER(S)

12. DISTRIBUTION/AVAILABILITY STATEMENT
Approved for public release; distribution is unlimited.

13. SUPPLEMENTARY NOTES
*Postgraduate Research Participation Program, Oak Ridge Institute for Science and Education, 4692 Millennium Dr., Suite 101, Belcamp, MD 21017

14. ABSTRACT
Development of efficient multifunctional structures is of interest for mass reduction of a variety of U.S. Army platforms. Structural batteries and supercapacitors are of particular interest for their ability to provide energy storage in load-bearing materials. Electrical separation of the electrode materials is required to prevent shorting and reduce self-discharge of the energy storage component. Polymer-based separator materials are typically used in traditional energy storage devices. For multifunctional composite applications this separator must also facilitate interlaminar bonding while maintaining chemical and physical compatibility. A series of potential inter-electrode separator materials, including a cellulosic paper, a microglass paper, and a porous polymer membrane, were investigated for adhesion, resistance, and lap shear strength. Vacuum-assisted resin transfer processing setups were used to fabricate composite-based supercapacitors. Throughout processing, resistance through the cells was monitored using a multimeter, and trends in resistance and overall resistivity were determined. Lap shear tests were conducted to better understand the effect each material would have on system strength as well as the separators' adhesion to the resin matrix and carbon fabric electrodes. The mode of failure for each material was also determined. The results of the experiments are instrumental in the determination of the proper electrical separator for use in structural energy storage devices. Initial testing on composite matrix and fiber-dominated properties, tensile modulus and short beam shear strength were also conducted. These experiments give significant insight into proper materials, processing methods, and testing protocols for the lab scale production of multifunctional structural batteries and supercapacitors.

15. SUBJECT TERMS
multifunctionality, composite, structure, energy storage device, processing

16. SECURITY CLASSIFICATION OF:			17. LIMITATION OF ABSTRACT	18. NUMBER OF PAGES	19a. NAME OF RESPONSIBLE PERSON
a. REPORT	b. ABSTRACT	c. THIS PAGE			James F. Snyder
Unclassified	Unclassified	Unclassified	UU	26	19b. TELEPHONE NUMBER (*Include area code*) 410-306-0842

Standard Form 298 (Rev. 8/98)
Prescribed by ANSI Std. Z39.18

Contents

List of Figures

List of Tables

INTENTIONALLY LEFT BLANK.

1. Introduction and Background

The performance of U.S. Army platforms is limited by the size and weight of conventional energy storage devices. A reduction in the weight and volume of energy storage devices could greatly benefit the capabilities of the Soldier as well as unmanned military vehicles. While research is being conducted to improve energy density of these devices, another approach is to enable other components of the overall platforms to be multifunctional; in particular, the structural components. Materials produced with structural integrity comparable to traditional load-bearing components that simultaneously provide electrochemical energy storage may help achieve system-level weight reduction (*1*, *2*).

Structural supercapacitors and batteries have been explored previously at the U.S. Army Research Laboratory (*3*–*5*) and elsewhere (*6*–*10*). One design for structural supercapacitors, the focus of this paper, can be seen in figure 1. The design merges the key element of an energy storage device and a fiber-reinforced polymer matrix composite. The supercapacitor consists of continuous-fiber fabrics reinforcing a resin matrix. Carbon fibers provide stiff structural reinforcement as well as a conductive surface for charge storage (*11, 12*). Lithium salt is added to the resin to create the electrolyte necessary for energy transfer between electrodes during charge or discharge while maintaining the requisite barrier to electron transport (*13*, *14*). Polar liquids can be added to facilitate ion mobility in the resin (*15*). The resin-based electrolyte also serves as the composite matrix (*4*). A thin membrane is often added to prevent interlaminar contact as a safeguard against the rapid self discharge of the stored energy that might occur if the electrodes short-circuit. However, this short-circuit safeguard may feasibly be addressed solely by the solid-state electrolyte if processed appropriately.

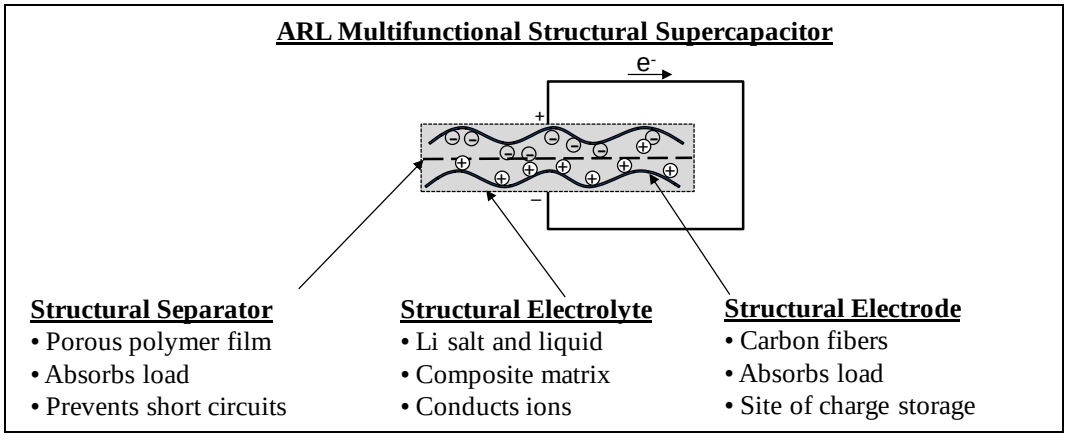

Figure 1. Structural supercapacitor diagram.

When a voltage potential is applied to the cell, the dissociated salt in the electrolyte matrix travels toward the fabric electrodes while electrons flow through the external circuit from one electrode to the other. The positive ions align along the surface of the electron-rich electrode in the form of an electrochemical double layer while the negative ions align along the electron-poor electrode in a similar manner. This charge separation enables the storage of electrical energy. The high surface area provided by some activated carbon fabrics can allow for energy storage orders of magnitude greater than in a traditional capacitor. Since there are no chemical reactions taking place, supercapacitors can be successfully cycled many more times than batteries without showing signs of degradation.

Given the complexity of designing structural composites that incorporate energy storage, there are several critical materials research areas that require attention. The research areas addressed in this report include the composite processing method, the impact of the separator material, and improving understanding of interfaces within the multifunctional composites. This paper specifically focuses on (1) processing limitations associated with structural gel electrolytes, and (2) the mechanical and electrical effects of using different types of interply separator materials in carbon-fiber laminates. In our previous studies with gel-type electrolytes, the processing of the composites has often resulted in undesirable macro-separation of liquid and resin. Elevated cure temperatures have also caused some problems with volatilizing of any liquid component of the electrolyte. Separator materials, required for adequate electrical isolation of the electrodes, have at times inhibited resin infiltration of the dry-stacked components as well as presented unquantified structural liabilities in the composite such as providing sites of delamination events in the composites. Voids, cracks, or other interfacial issues related to the separator can also affect charge transport within the composite. All of these topics remain subjects of active interest.

2. Experiment and Calculations

2.1 Materials

Carbon fabrics investigated as electrodes included T300–3K plain weave carbon fabric obtained from Textile Products, Inc., and Spectracarb Activated Carbon Fabric Type 2225 obtained from Engineered Fibers Technology, LLC.

Materials formally investigated as separators included Celgard 3501 polymer membrane obtained from Celgard LLC, BG 03015 nonwoven microglass battery-pasting paper obtained from Hollingsworth and Vose, and Kraft paper. Informal studies were also performed on a wider range of materials, including Fibre Glast part 573-B and Fiberglassite fiberglass, AFN-grade 8000111 hot-pressed glass fiber, Whatman nos. 41 and 42 ashless filter paper, VWR-brand glass microfiber filter paper no. 691, and Celgard 2500 polymer membrane.

The structural electrolytes in this study comprised a structural resin, a liquid solvent, and a lithium salt. Tetraethylene glycol dimethacrylate (Sartomer Corp., code SR209) was investigated as the representative structural resin. It was polymerized at room temperature using anhydrous propylene carbonate (PC); (Sigma Aldrich) as the representative liquid electrolyte solvent. Lithium trifluromethanesulfonimide (LiTFSI); (3M Fluorad) was used as the lithium salt.

All materials used in preparation of the structural electrolyte were handled in a glove box under a dry nitrogen atmosphere. A baseline liquid electrolyte solution was prepared by dissolving 1-M LiTFSI in PC. The solution was dried over 4-Å activated molecular sieves. The structural electrolyte precursor was prepared by mixing the proper ratio of resin monomer and liquid electrolyte and adding 1.5-wt % Trigonox 239 (Akzo Nobel Chemicals) as the radical initiator and 2% cobalt naphthenate (CoNap); (Sigma Aldrich) as a catalyst to facilitate curing at room temperature. The solution was transferred from the mixing container into a 50-mL plastic syringe and brought outside of the glove box to be used immediately.

2.2 Composite Assembly and Processing

2.2.1 Samples for Electrical and Lap Shear Testing

Structural supercapacitors were processed and fabricated using vacuum-assisted resin transfer molding (VARTM). Stacks were generated by alternating a single ply of carbon fabric with the desired number of separator plies. For the initial wet-out tests, stacks of five carbon/separator plies were compiled and processed. Each piece of material was 5 in wide ×5 in long. The next wave of composite layups was designed based on the ASTM Standard Test Method for Lap Shear Adhesion for FRP Bonding (D 5868) (*16*). The fabric and separators were cut and assembled to the specifications illustrated in figure 2.

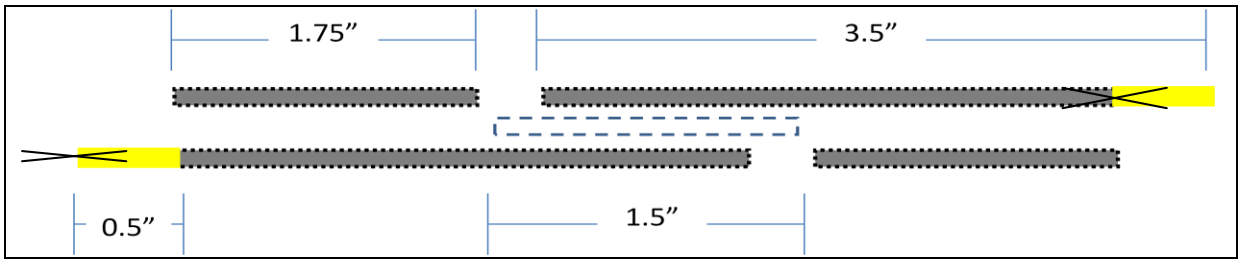

Figure 2. Composite layup diagram.

The black boxes in figure 2 depict carbon fabric, the dashed box depicts the separator, and the 1/2-in solid boxes with Xs at the ends depict copper tape folded over the ends of the carbon fabric for electrical testing purposes. The length of carbon fabric overlap in the lap shear area was 1 in. Excluding the copper tape, the samples were a total of 5 in long. Additional copper tape was attached perpendicular to the copper tape end tabs, extending out from the VARTM setup to enable in-situ electrical measurements as shown in figure 3. Initial layups consisted of fabrics

that were 2 1/2 in wide with separators that were 3 in wide in an attempt to prevent shorting. The layups used in the resistivity tests consisted of separators that were 5 in wide. These layups were processed three at a time in a VARTM setup as shown in figure 3.

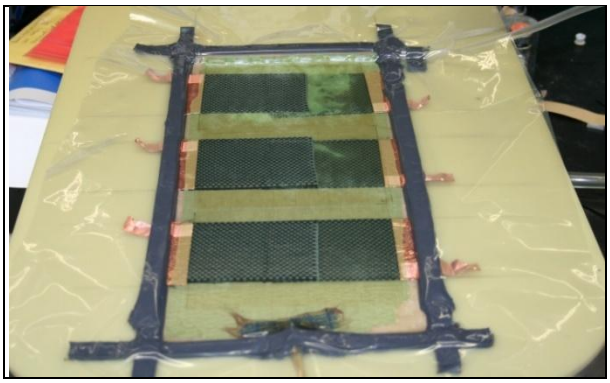

Figure 3. Typical VARTM setup.

After the processing technique had been adequately developed, layups consisted of fabrics that were 5 1/2 in wide with 6 1/2-in-wide separators. These layups were processed two at a time in each VARTM setup. Typically, 30 g of resin were needed to successfully inject the entire mold. The exact amount of resin used in each mold varied; however, injection was stopped once the entire mold had been filled with the resin.

VARTM setups were constructed on fiberglass caul plates to prevent electrical shorting through the caul plate and to allow resistivity to be tested throughout the curing process of the part. A Teflon-coated release ply (RE234 TFNP50; Airtech International) was used as the bottom layer to prevent resin adhesion to the part or plate. Tacky Tape* was used to create a seal capable of maintaining a sufficient vacuum. The vacuum line (a length of plastic tubing with alternating slits that spans the width of the setup), resin injection line (a length of tubing equal to the width of the setup with one end placed 0.5 in into the mold on the opposite end of the setup), and copper tabs from each layup were pressed on top of the first layer of tape. A second layer of tape was applied to create a seal between the inlet line, outlet line, copper tabs, and nylon vacuum bag (WN 1500; Airtech) that was used to seal the entire setup. A 710-mm mercury vacuum was applied to ensure proper sealing of the mold and for the infusion process.

Cure schedules were closely monitored for each laminate. The composite panels processed with 100% Sartomer SR209 resin were allowed to cure at room temperature for 16 h under vacuum and post cured at 70 °C for 1 h under vacuum. Composites containing gel matrices were cured for 16 h at 70 °C under vacuum. Once the cure schedule was completed, the vacuum was released from the mold and the parts were cut out. The copper tape tabs sticking out of the bag were cut off with a razor blade during the removal process.

* Tacky Tape is a registered trademark of Schnee-Morehead, Inc., Irving, TX.

2.2.2 Samples for Tensile and Short Beam Shear Testing

Tensile and short beam shear mechanical testing layups were prepared on glass tool surfaces. The fabric stack was assembled directly on the tool surface. A single sheet of release ply was placed on top of the layup followed by a distribution media that covered most of the carbon layup. The remainder of the VARTM process was identical to that described in the previous section. The T300 tensile test laminates comprised 10 plies of 12- × 12-in T300 with two plies of equal size Celgard 3501 between each pair of carbon fabrics to produce laminates 0.1 in thick. The T300 short beam shear test laminates comprised 26 plies of 6- × 8-in T300 with two plies of Celgard 3501 separating only the middle two plies of carbon fabric. The Spectracarb layups were the same size and construction except that 6 and 18 plies of carbon fabric were used for the tensile and short beam shear specimens, respectively. The matrices comprised SR 209 structural resin in combination with 0%–50% propylene carbonate-based liquid electrolyte.

2.3 Characterization

2.3.1 Resistivity Testing

Resistivity tests were conducted throughout the entire curing process. A Fluke 187 multimeter was used to read the resistance of each part. Resistances were taken (1) for each part dry under vacuum, (2) immediately following resin injection, (3) following post cure, (4) after the part had been removed from the mold, and (5) while the removed part had 5 psi of pressure on the lap shear joint.

2.3.2 Lap Shear Testing

Lap shear test specimens were generated by cutting the appropriate laminate into 1-in-wide strips using a table saw or ceramic scissors. The exact dimensions of the overlap area were measured using Mitutoyo Absolute Digimatic calipers. Lap shear tests were run on an Instron 1123 load frame with a 1000–lbf load cell at 0.5 in/min based on the ASTM 5868 standard (*16*). The maximum strength was determined by dividing the maximum applied load by the lap shear area. The type of failure was determined visually. An optical microscope at 100x magnification was also used as necessary. Failure types included adhesive failure, cohesive separator failure, and fiber tear of electrodes.

2.3.3 Tensile Testing

Tensile tests were performed using an Instron 1125 load frame with a 10,000-lb load cell on samples based on the ASTM 3039 standard (*17*). Specimens were cut from the appropriate laminate using a diamond-tipped table saw. T300 tensile specimens were tabbed with 1- × 2-in fiberglass tabs adhered with Henkel Hysol 9309 two-part epoxy adhesive. Spectracarb samples were not tabbed in the grip area; rather, 40-grit sandpaper was used to ensure that slipping did not occur.

Digital image correlation was used to measure strain. The tool side of each specimen was spray-painted white with ColorPlace spray paint. Black spray paint was then speckled on to the white surface with dots approximately 0.05 in diameter and with a dot density of 400 dots/in^2. Pictures were taken with a high-speed camera and recorded using Vic-Snap software at a rate of one picture every 4 s. The raw data was correlated and the strain was calculated using the Vic2D software. Between 5 and 10 specimens were tested for every sample.

2.3.4 Short Beam Shear Testing

Short beam shear tests were performed using an Instron 1125 load frame with a 1000-lb load cell based on the ASTM 2344 standard (*18*). A short bear-shear apparatus containing a micrometer-controlled span width and an automatic sample centering device were used in sample testing. To qualify for desired analysis, short beam shear samples must have failed between the middle plies of the laminate. The short beam shear strength calculated for samples that fail in this manner directly correlates to the interlaminar strength of the composite. Between 5 and 10 specimens were tested for every sample.

2.3.5 Cure Schedule Determination

Structural electrolyte gels containing greater than 50% liquid electrolyte demonstrated an inability to cure properly in composites using the cure schedule determined in previous studies (16 h at 70 °C). This was hypothesized to be a function of the volatilization of the PC at elevated temperatures and vacuum conditions present during VARTM processing in thin films and on high surface area fabrics. Two plies of T-300 measuring 3 in long × 2 in wide, separated by one ply of Celgard 3501 membrane, were wet-out with 1 g of uncured gel electrolyte and placed on a glass slide. Electrolyte compositions investigated ranged from 10% to 90% PC. The samples were held at 22, 40, and 80 °C until fully cured as determined by visual inspection. At that point the mass loss was determined and samples were peeled apart to determine if adhesion between the layers existed

3. Results

3.1 Downselection of Separator Material

Separator testing was performed to downselect an appropriate material as based on two important properties: interlaminar resistance through the separators and modified lap shear strength.

3.1.1 Separator and Laminate Wet-Out

Each separator in this study was tested for rate of absorption of vinyl ester resin and PC. Although resin absorption was not rapid, it was fast enough that laminates were expected to fully wet-out before the matrix viscosity increased substantially. Initial tests using laminate

configurations, and subsequent inspection by peeling each layer off, indicated that all layers of carbon fabric and separator were successfully infiltrated by the resin.

3.1.2 Resistivity

Inter-electrode electrical resistance through the separators was measured during each of the five stages of the VARTM process. Resin was used without salt in to order to minimize the number of free charge carriers and more accurately identify the presence of electrical shorting. The number and type of separator used in each sample is listed in table 1 along with the resistance of each laminate and the time at which the measurement was taken. A pressure of 5 psi was applied to each laminate after removal from the mold for the "Final Part w/Pressure" resistance measurement. The resistance was often retested without pressure following this measurement, and it had always returned to the "Final Part" value, which indicates that the changes in resistivity are related to small changes in interfacial contacts and/or interlaminar proximity rather than permanent changes to the microstructure. The infinity symbols show no reading detected by the multimeter, indicating a negligibly small conductivity through the composite.

Table 1. Resistivity data for different separator types and quantities at each stage in laminate formation process.

Type of Separator	**Resistance (ohms)**				
	Dry Under Vacuum	**After Injection**	**After Post Cure**	**Final Part**	**Final Part w/ Pressure**
No Separator	3.8×10^{1}	3.1×10^{1}	4.4×10^{1}	4.3×10^{1}	2.9×10^{1}
Celgard 1 Ply	1.9×10^{6}	1.1×10^{4}	1.0×10^{8}	∞	1.1×10^{7}
Celgard 2 Ply	2.7×10^{6}	4.9×10^{4}	∞	∞	6.8×10^{6}
Celgard 3 Ply	4.5×10^{6}	1.1×10^{6}	∞	∞	1.2×10^{7}
BG 1 Ply	6.7×10^{2}	5.7×10^{2}	1.5×10^{6}	∞	∞
BG 2 Ply	6.1×10^{6}	1.8×10^{4}	1.9×10^{6}	∞	2.7×10^{6}
BG 3 Ply	6.9×10^{6}	5.3×10^{4}	6.2×10^{6}	∞	3.1×10^{6}
Kraft 1 Ply	1.2×10^{8}	1.5×10^{6}	7.9×10^{7}	1.3×10^{7}	1.1×10^{7}
Kraft 2 Ply	3.9×10^{8}	2.4×10^{6}	6.8×10^{7}	9.5×10^{6}	8.9×10^{6}
Kraft 3 Ply	5.2×10^{8}	2.7×10^{6}	1.1×10^{8}	1.3×10^{7}	8.2×10^{6}

The data in table 1 indicate that for the materials studied here the number of separators has a small but meaningful impact on inter-electrode resistance, while the type of separator and stage of processing each has a much more substantial (orders of magnitude) effect on inter-electrode resistance. This result is encouraging since it suggests that with careful processing laminates may require only one separator ply to maximize resistive efficiency, enabling a minimization of

interelectrode spacing and matrix volume fraction. Some incongruous variability in the data for the cured stages, and the low resistances measured for one-ply BG 03015, suggest that it would be wise to include two plies of material to ensure electrical isolation.

Addressing the data at each processing stage in more detail, two interesting and consistent behaviors are evident. The first is that a significant decrease in resistance was noted for all samples during resin injection. This change is unlikely to result solely from residual ion content in vinyl ester resins, as it is typically very small as verified by conductivity tests of the liquid resin that demonstrated very high bulk resistivities. Under direct current bias the ionic conductivity should diminish over time, which it did not. The source of this anomaly may instead reflect better formation of the interfaces during the liquid stage versus the prior evacuated stage or ensuing solid phase. After cure the resistance increased substantially, further suggesting possible reliance on interfacial charge transfer. The second curious behavior, which may also relate to interfaces, is the convergence of all of the sample data to approximately the same resistance when pressure is applied during the last measurement. This is notable since the Celgard 3501 and BG 03015 samples had greater than 1 gigaohm resistance in the final part under atmospheric pressure. One possibility is that voids are formed during cure with much higher resistivity than the bulk polymer. Additional force exerted on the laminate may close these gaps off, enabling the inherent resistance of the bulk polymer. Kraft paper was not found to exhibit a spike in resistivity, which may indicate better interface formation during cure.

3.1.3 Lap Shear Strength

Lap shear tests provided insight into the quality of adhesion between the separator and the matrix. Figure 4 illustrates the maximum lap shear strength for T300 using each of the three separators. Two plies of separator were used between carbon plies in this study to ensure electrical isolation. Laminates without interstitial separators are included for comparison. Each sample consists of five specimen runs. Each separator is statistically different according to the standard deviation of the data.

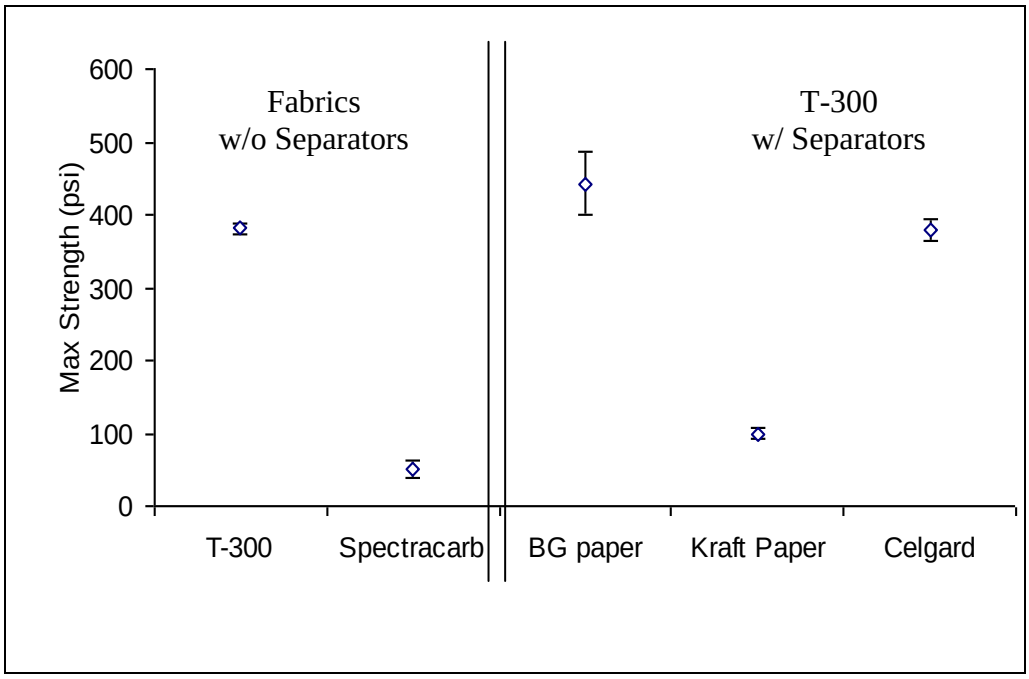

Figure 4. Lap shear strength of different separator materials.

Lap shear data for one, two, and three plies of the Celgard and BG separators between T300 plies are presented in figure 5. Kraft paper was not pursued in this follow-on study due to its poor lap shear strength in figure 4. The zero-ply data point in figure 5 is a T300 baseline sample that does not contain a separator. The two-ply sample data were determined from five specimens as specified in the ASTM standard *(16)*, while the one- and three-ply sample data were determined from only two specimens.

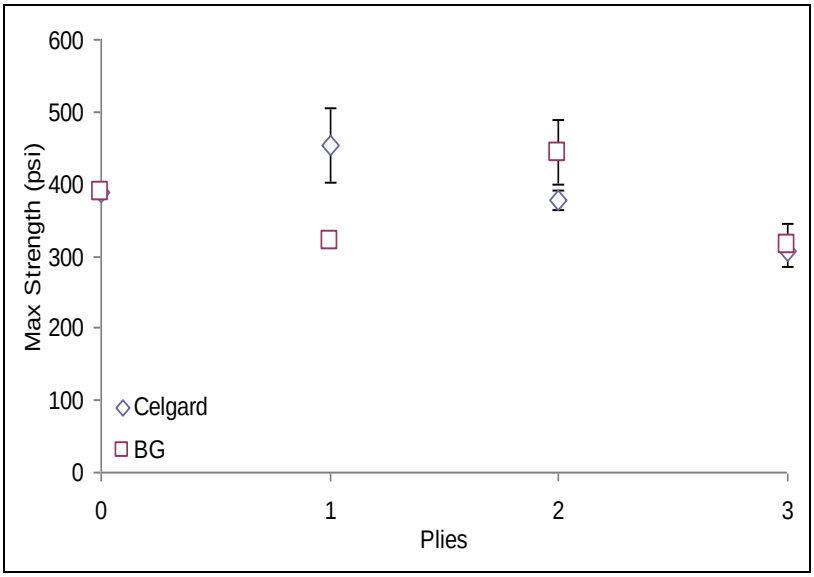

Figure 5. T300 lap shear strength for different numbers of plies of separator.

Three types of failure were identified following lap shear test completion. Results were mostly determined manually or under visual magnification. A table summarizing the types of failure is shown in table 2. Adhesive failure typically occurred primarily in the matrix and demonstrated little damage to the fabric or separator layers. Cohesive failure occurred in the separator and suggested sufficient adhesion between the separator and matrix but low resistance to tearing in the separator. The Celgard 3501 and BG 03015 samples were evaluated after tests associated with both figures 5 and 6, and they all failed as described in table 2 regardless of the number of separators. The Celgard/BG/Celgard and BG/Celgard/BG types were sandwich structures comprising the three separator plies to elucidate more insight into the failure mechanism for the Celgard 3501 and BG 03015. The Spectracarb samples all failed cohesively above or below the lap shear area rather than in the area of overlap.

Table 2. Summary table of observed failure types.

Separator	Failure Type	Failure Interface
None (T300 baseline)	Adhesive	T300/T300
None (2225 baseline)	Fiber tear	—
2 plies Kraft Paper	Cohesive	—
2 plies Celgard 3501	Cohesive	—
2 plies BG 03015	Adhesive	BG/T300
Celgard/BG/Celgard	Adhesive	Celgard/BG
BG/Celgard/BG	Adhesive	Celgard/BG

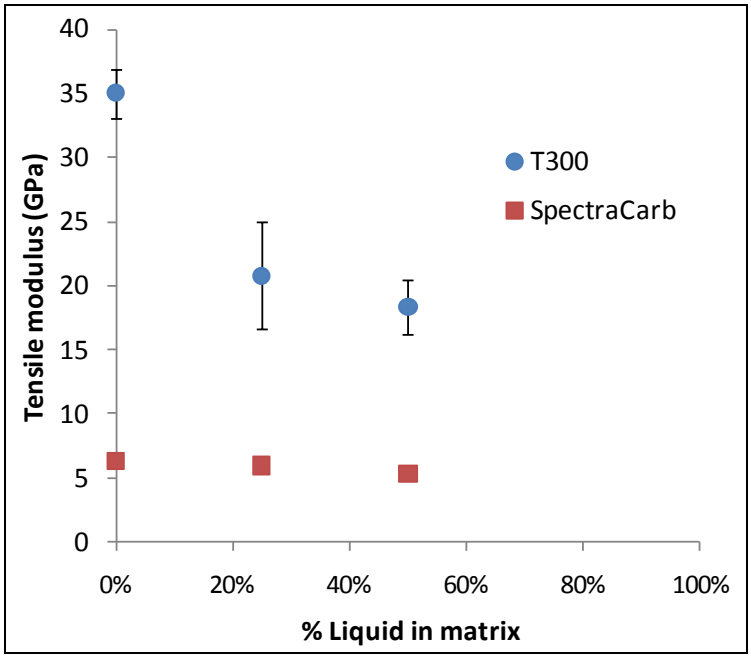

Figure 6. Tensile modulus for structural supercpacitors with structural gel electrolytes.

The separators are expected to worsen the mechanical properties since they are not load bearing, not strong in flexure, and reduce structural fiber volume of the composites. However, figures 5 and 6 suggest that inclusion of up to three plies of the BG 03015 or Celgard 3501 separator materials does not significantly reduce the lap shear strength in a T300 laminate.

3.2 Determination of Cure Schedule

Previous studies on gel-type structural electrolytes in our laboratory have focused on bulk materials to study ion conductivity and mechanical properties. To evaluate the processing behavior of these materials in a laminate configuration, a series of tests were prepared to elucidate the impact of including a liquid solvent in the structural electrolyte with respect to matrix formation, interlaminar adhesion, and solvent retention.

The results are listed in table 3. As expected, at 80 °C a significant amount, up to 83%, of the electrolyte evaporated during the curing process. As a result, a cohesive matrix was not formed and no adhesion was detected in samples containing 50% or more PC. At 40 °C and room temperature there was less evaporation of electrolyte, and samples containing up to 70% PC demonstrated interlaminar adhesion at extended cure times even though approximately 10% of the electrolyte was lost in each case.

Table 3. Solvent loss and gel cure as a function of cure temperature and time.

% PC in Resin	PC Mass (g)	80 °C – 16-h cure			40 °C – 40-h cure			22 °C – 88-h cure		
		Mass Loss (g)	PC Mass loss	Adhesion	Mass Loss (g)	PC Mass Loss	Adhesion	Mass Loss (g)	PC Mass Loss	Adhesion
100%	1.0	0.74	74%	—	0.47	47%	—	0.26	26%	—
90%	0.9	0.71	79%	—	0.42	47%	—	0.17	19%	—
70%	0.7	0.58	83%	—	0.08	11%	×	0.11	16%	×
50%	0.5	0.20	40%	—	0.06	12%	×	0.08	16%	×
30%	0.3	0.09	30%	×	0.02	7%	×	0.04	13%	×
10%	0.1	0.02	20%	×	0.01	10%	×	0	0%	×

Note: "×" indicates samples that did demonstrated adhesion.

3.3 Preliminary Composite Mechanical Properties

3.3.1 Tensile Tests

The tensile properties of structural supercapacitor laminates were evaluated to gauge the relative impact of fiber type on composite performance. Figure 6 illustrates the results and figure 7 shows images from the tests. The calculated tensile modulus is plotted as a function of electrolyte percentage for both fabrics tested. The standard deviation is shown on the plot. As expected, the tensile modulus was dominated by fiber properties with the T300 consistently outperforming the 2225 fibers across all matrix compositions. The failure mode for the 2225 samples was fiber tear

in the gauge length, indicating fiber-dominated properties, a conclusion further validated by the minimal variation observed in modulus relative to matrix composition. The failure mode for the T300 samples was interlaminar failure, indicating some matrix dependency or adhesion issues, which is also evident in the slight decline in modulus with increased liquid percentage.

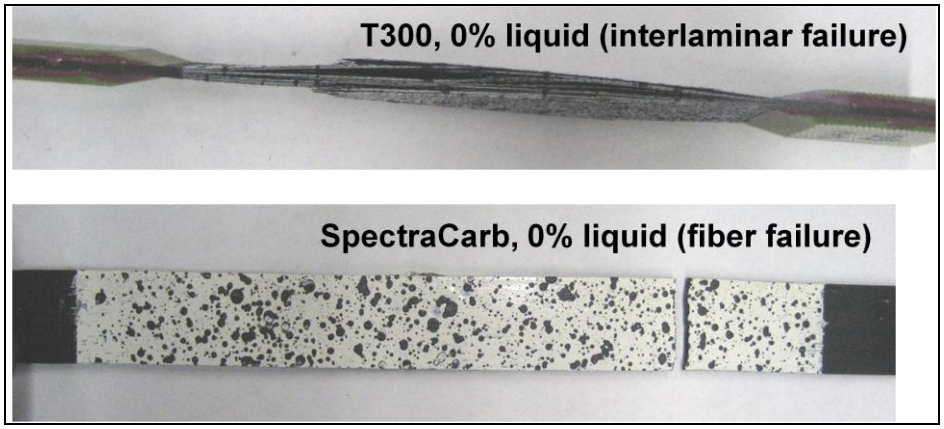

Figure 7. Images of tensile test specimens.

3.3.2 Shear Testing

The interlaminar strength of the composites was tested via the short beam shear method. Failure occurred in the desired planes for these samples. The calculated short beam shear strength is illustrated in figure 8 as a function of electrolyte percentage for both fabrics tested. The standard deviation is shown on the plot. Figure 9 shows sample images for T300. The composite exhibited interlaminar failure in the desired planes between the middle plies of Celgard membrane where the stress state is primarily shear. Failure initiated at the edge of the laminate and propagated through the width.

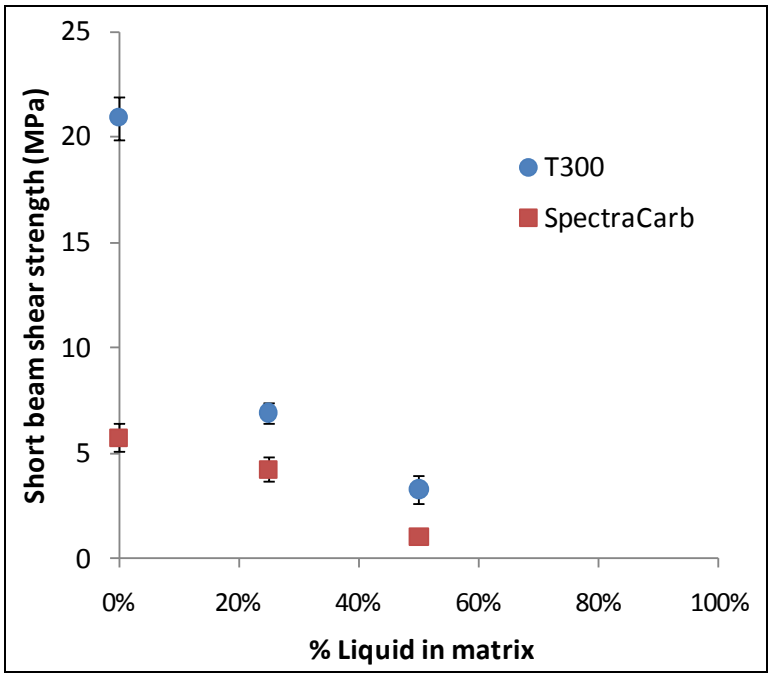

Figure 8. Short beam shear strength for structural supercpacitors with structural gel electrolytes.

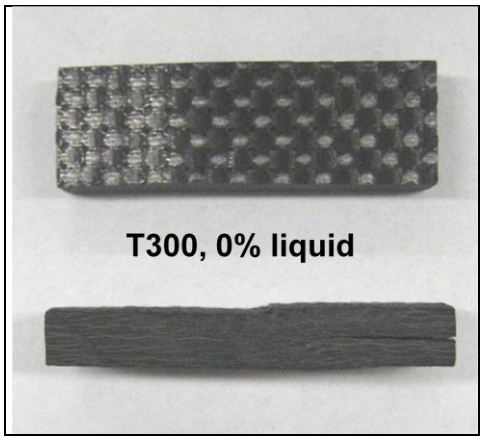

Figure 9. Images of short beam shear test specimen for T300.

Shear strength was found to decrease dramatically with increased liquid electrolyte concentration, as expected. For the 100% structural resin specimens, the shear strength of the T300 specimen is five times greater than the 2225 specimen due to greater fiber stiffness of the former. However, at higher liquid concentrations, the shear strength becomes much more dependent on matrix composition and less on fiber type.

4. Summary and Conclusions

Successful structural energy storage devices present potential mass benefits to U.S. Army platforms. Two material aspects were evaluated in this study. The first is the impact of the inter-electrode electrical separator on cell resistance and shear properties and the second is the impact of cure schedule on solvent retention in gel-type structural electrolytes. Both of these studies are critical to improving structural devices based on laminate configurations, including structural batteries and structural supercapacitors.

Materials providing for inter-electrode electrical separation are necessary to minimize electrical shorting; however, these materials are anticipated to reduce the mechanical properties since they typically are not load bearing, not strong in flexure, and reduce structural fiber volume in the composites. Three material types were studied here: a cellulosic paper (Kraft paper), a microglass paper (BG 03015), and a porous polymer membrane (Celgard 3501). All of these materials can be lightweight and adaptable to composites applications, and each separator material appeared to wet out with resin. BG 03015 and Celgard 3501 exhibited similar interfacial strength in resin, and both outperformed Kraft paper. Both also exhibited similar trends in providing interfacial resistance with each stage of processing, although BG 03015 demonstrated lower overall resistance and possible indications of charge leakage.

Ultimately, the polymer membrane was downselected for continuing tests since it is more effectively designed for safety and performance attributes appropriate to energy storage device applications. Further studies are anticipated to determine the possibility of using only one ply of polymer membrane to minimize parasitic mass in the device, improve mechanical properties at the interfaces, and increase fiber volume of the electrodes.

Laminate cure studies indicated the importance of maintaining a relatively low temperature and short time at temperature during processing, even for high boiling point solvents, to minimize solvent loss. Thermal treatment at 40 °C was not found to be significantly worse for solvent retention than room temperature polymerizations, and the small solvent loss percents were determined to be acceptable for the intended applications.

The preliminary tensile and interlaminar shear strengths were studied using Celgard 3501 as separator as determined in section 3.1 and the cure schedule determined in section 3.2. Laminates were manufactured with a range of structural resin/liquid electrolyte combinations that demonstrated the mechanical viability of these composites. Future investigations include study of larger laminates constructed using 10 stacked carbon fabrics (nine supercapacitor cells). Further study of the solid interfaces and void composition are also anticipated.

5. References

1. Wetzel, E. Multifunctional Structural Composite Materials for U.S. Army Applications. *AMPTIAC Quarterly* **2004**, *8* (4), 91–95.

2. O'Brien, D. J.; Baechle, D. M.; Wetzel, E. D. Design and Performance of Multifunctional Structural Composite Capacitors. *Journal of Composite Materials* **2011**, *45* (26), 2797–2809.

3. Gienger, E. B.; Snyder, J. F.; Wetzel, E. D.; Xu, K. Multifunctional Structural Composite Development and Evaluation. *Proceedings of the Society for Advancement of Material and Process Engineering*, Baltimore, MD, 21-24 May, 2012.

4. Snyder, J. F.; Gienger, E. B; Wetzel, E. D.; Xu, K. Energy Density and Rate Limitations in Structural Composite Supercapacitors. *Proceedings of the SPIE – The International Society for Optical Engineering*, Baltimore, MD, April 2012; Vol. 8377, Article 837709.

5. Snyder, J. F.; Baechle, D. M.; Wetzel, E. D.; Xu, K. *Structural Composite Batteries and Supercapacitors*; ARL-TR-5328; U.S. Army Research Laboratory: Aberdeen Proving Ground, MD, 2010.

6. Gallagher, T.; LaMaster, D.; Ciocanel, C.; Browder, C. Electro-Mechanical Characterization of Structural Supercapacitors. *Proceedings of SPIE – The International Society for Optical Engineering*, San Diego, CA, March 2012; Vol. 8342, Article 83420S.

7. Shirshova, N.; Qian, H.; Shaffer, M. S. P.; Steinke, J. H. G.; Greenhalgh, E. S.; Curtis, P. T.; Kucernak, A.; Bismarck, A. Structural Composite Supercapacitors. *Composites Part A-Applied Science and Manufacturing* **2013**, *46*, 96–107.

8. Ekstedt, S.; Wysocki, M.; Asp, L. E. Structural Batteries Made From Fibre Reinforced Composites. *Plastics, Rubber and Composites* **2010**, *39* (3/4/5), 148–150.

9. Liu, P.; Sherman, E.; Jacobsen, A. Design and Fabrication of Multifunctional Structural Batteries. *Journal of Power Sources* **2009**, *189* (*1*), 646–650.

10. Thomas, J. P.; Qidwai, M. A. The Design and Application of Multifunctional Structure-Battery Materials Systems. *JOM Journal of the Minerals, Metals and Materials Society* **2005**, *57* (3) 18–24.

11. Kjell, M. H.; Jacques, E.; Zenkert, D.; Behm, M.; Lindbergh, G. PAN-Based Carbo Fiber Negative Electrodes for Structural Lithium-Ion Batteries. *J. Electrochem. Soc.* **2011,** *158*, (12), A1455–A1460.

12. Snyder, J. F.; Wong, E. L.; Hubbard, C. W. Evaluation of Commercially Available Carbon Fibers, Fabrics, and Papers for Potential Use in Multifunctional Energy Storage Applications. *Journal of the Electrochemical Society* **2009**, *156* (3), A215–A224.

13. Snyder, J. F.; Carter, R. H.; Wetzel, E. D. Electrochemical and Mechanical Behavior in Mechanically Robust Solid Polymer Electrolytes for Use in Multifunctional Structural Batteries. *Chemistry of Materials* **2007** *19* (15), 3793–3801.

14. Snyder, J. F.; Wetzel, E. D.; Watson, C. M. Improving Multifunctional Behavior in Structural Electrolytes through Copolymerization of Structure-and Conductivity-Promoting Monomers. *Polymer* **2009**, *50*, (20), 4906–4916.

15. Nguyen T.; Snyder, J. Multifunctional Properties of Structural Gel Electrolytes. *ECS Transactions* **2008**, *11 (*32), 73–83.

16. ASTM D 5868. Standard Test Method for Lap Shear Adhesion for Fiber Reinforced Plastic (FRP) Bonding, *Annu. Book ASTM Stand.* **2008**.

17. ASTM D 3039/D 3039M. Standard Test Method for Tensile Properties of Polymer Matrix Composite Materials, *Annu. Book ASTM Stand.* **2008**.

18. ASTM D 2344/D 2344M. Standard Test Method for Short-Beam Strength of Polymer Matrix Composite Materials and Their Laminates, *Annu. Book ASTM Stand.* **2006**.

NO. OF
COPIES ORGANIZATION

1 (PDF) DEFENSE TECHNICAL INFORMATION CTR DTIC OCA

1 (PDF) DIRECTOR US ARMY RESEARCH LAB IMAL HRA

1 (PDF) DIRECTOR US ARMY RESEARCH LAB RDRL CIO LL

1 (PDF) GOVT PRINTG OFC A MALHOTRA

ABERDEEN PROVING GROUND

2 (PDF) RDRL WMM G
E GIENGER
J SNYDER

1 (PDF) RDRL WMM A
E WETZEL

INTENTIONALLY LEFT BLANK.